Study of Antennas for a Low Cost Interferometer

Dimas Irion Alves [1], Nelson Jorge Schuch [1], Natanael Rodrigues Gomes [2],Guilherme Simon da Rosa [3], Ândrei Camponogara [1], Cláudio Machado Paulo [1].

[1] Southern Regional Space Research Center - CRS/CCR/INPE - MCT in collaboration with the Santa Maria Space Science Laboratory - LACESM/CT - UFSM, Santa Maria, RS, Brazil, (dirion@lacesm.ufsm.br); [2] Electronic and Computing Department and Santa Maria Space Science Laboratory, ((DELC-LACESM)/CT/UFSM), Santa Maria, RS, Brazil; [3] Center for Telecommunications Studies, Catholic University of Rio de Janeiro (CETUC/PUC- RIO), Rio de Janeiro, RJ, Brazil.

This paper was prepared for presentation at the Twelfth International Congress of the Brazilian Geophysical Society, held in Rio de Janeiro, Brazil, August 15-18, 2011.

Abstract

The project of a modern interferometric array similar to the Low Frequency Array (LOFAR) Prototype Station (LOPES), to cover the LOFAR frequency range under 100 MHz is being developed at the Southern Space Observatory (SSO, 29.4^{o} S, 59.4^{o} W), São Martinho da Serra, RS, Brazil. Therefore, it is necessary to study different kinds of antennas that cover the large proportions of the interferometer necessity. The large number of antennas required for a LOFAR like interferometer suggests that the antenna design must have: a low development cost, avoid complex mechanical structures, robust mechanical facilities, and a large useful bandwidth dominated by the Galactic radio noise, in order to maintain a low station cost. This work presents a study of four kinds of antennas designs (NLTA, Inverted-V dipole, Fork and Half-wavelength dipole), the results of antennas simulations comparisons using the NEC-2 software and finally for each antenna a cost-benefit analysis.

Introduction

The Low Frequency Array (LOFAR) is the next generation radio telescope which uses the phased antenna array concept to form an aperture synthesis telescope which receives signals of radio in the frequency range from 10 to 250 MHz, with about 10,240 dipoles polarized (Tan et al, 2000; Astron, 2011). The project has as main research lines: extragalactic research, transient sources, high-energy cosmic rays, space weather and solar science, space magnetism, among other (Lofar, 2011).

To verify if the cosmic ray emissions are detectable and useable in an observational site region, the LOFAR Prototype Station (LOPES) was built, which is, basically, a dipole antennas array, developed for testing some LOFAR concept aspects (Rosa et al, 2010a).

An interferometer using a similar LOPES's methodology is in development in the Southern Space Observatory (SSO), as shown Figure 1. According to (Ellingson, 2005), the antennas must have a development low cost, a mechanically simple and resistant structure and a large bandwidth dominated by the Galactic radio noise. Also (Ellingson, 2005) shows that even simple dipoles can deliver a high useable bandwidth for frequencies under 100 MHz, when the telescope sensitivity is limited by the Galactic radio noise.

This work has studied four kinds of antennas designs: 1) the Naval Research LOFAR Test Array (NLTA), proposed by (Ellingson, 2005; Stewart et al, 2004), 2) Inverted-V dipole proposed by (Capellen et al, 2007) and using the optimizations proposed by (Rosa, 2010b), 3) Fork Antenna using the optimizations proposed by (Rosa, 2010b) and 4) a single Half-wavelength dipole for the 50 MHz frequency.

Figure 1: Inverted-V dipoles used in the interferometer installed in the Southern Space Observatory (SSO).

Method

The method used was divided into the following sub-sections: simulation parameters, active antenna, Galactic radio noise model, useful bandwidth, NLTA antenna, Inverted-V dipole, Fork antenna and Half-wavelength dipole.

Simulation Parameters

The simulations were performed using the NEC-2 software, considering a realistic lossy ground scenario with conductivity of σ = 5 mS/m and relative permittivity of

ε_r = 13, environmental temperature of 290 K, preamplifier noise temperature of 360 K. The assumed impedance value in the preamplifier input was 100 Ω. The transmission line considered was 100 m coaxial cable RG-58 with gain associated with the transmission ranging from -4.8 dB to -15.6 dB between the frequencies of 10 MHz to 100 MHz. It was used the instrumental noise analysis procedure of (Ellingson, 2005; Rosa, 2010c), neglecting the antennas polarization and it was used a superestimated approximation of the Galactic radio noise temperature model proposed by (Cane, 1979).

Active Antenna

The active antennas were initially conceived as receiving antennas for frequencies below 30 MHz, where the external noise exceeds the instrumentation noise (Tan et al, 2000).These antennas are based on the fact that reducing the radiator length of a tuned antenna does not affect the signal to noise ratio at the antenna output, since the external radio noise level is even stronger than the internal (Tan et al, 2000).

An active antenna for a radio telescope operating at low frequencies can be generically modeled using three basic parameters: 1) the antenna radiator, 2) the active balun (balance to unbalanced transformer), that is a preamplifier located near the antenna radiator, and 3) the transmission line connecting the balun to the receiver input (Rosa, 2010c).

The block diagram of Figure 2 shows a simplified active antenna configuration used in the interferometer installed at the SSO.

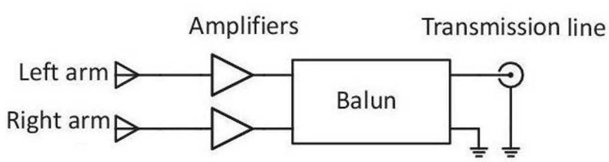

Figure 2: Basic diagram of the antenna used in the SSO.

Galactic Radio Noise Model

The Galactic radio noise power is described in terms of intensity I_ν integrated over the antenna pattern. The power spectral density at the antenna terminals is calculated by

$$S_a \approx \frac{1}{2}\int I_\nu A_e d\Omega \; [W\ Hz^{-1}] \tag{1}$$

Where A_e is the antenna effective aperture, the integration is over a solid angle Ω and the factor $1/2$ is, because any single polarization captures about half of the available power, considering the Galactic radio noise unpolarized (Ellingson, 2005).

The Galactic radio noise intensity can be modeled as being uniform in the space and filling the antenna beam. It is necessary that the antennas used in this application have a large beamwidth, A_e is almost constant in over the sky (Ellingson, 2005). Thus, we can simplify (1) to

$$S_a \approx \frac{1}{2} I_\nu A_e \Omega \; [W\ Hz^{-1}] \tag{2}$$

Assuming that the antenna gain is very small, at and below the horizon. Where Ω is a beam solid angle.

The antenna gain is given by

$$G = e_r D \tag{3}$$

Where D is the directivity and e_r is the antenna efficiency. In this analysis, mechanisms which make $e_r < 1$ include loss due to the finite conductivity of the materials used to make the antenna, and the imperfect ground (Ellingson, 2005). Using

$$A_e = \frac{\lambda^2}{4\pi} G \text{ and } \Omega = \frac{4\pi}{D} \tag{4}$$

(2) can be simplified to

$$S_a \approx \frac{1}{2} e_r I_\nu \frac{c^2}{\nu^2} \tag{5}$$

Where c is the speed of the light and ν is the frequency. The intensity I_ν can be expressed as equivalent temperature using the Rayleigh-Jeans law

$$I_\nu = \frac{2\nu^2}{c^2} k T_{sky} \tag{6}$$

Where k is the Boltzmann constant ($1.38 \times 10^{-23}\ J/K$) and T_{sky} is the antenna equivalent temperature corresponding the Galactic radio noise. Then (5) can be described by

$$S_a \approx e_r k T_{sky} \tag{7}$$

and

$$T_{sky} = \frac{1}{2k} I_\nu \frac{c^2}{\nu^2} \tag{8}$$

An approximation for $I\nu$ can be obtained from (Cane, 1979)

$$I_\nu = I_g \nu^{-0.52} \frac{1 - e^{-\tau(\nu)}}{\tau(\nu)} + I_{eg} \nu^{-0.80} e^{-\tau(\nu)} \tag{9}$$

Where $I_g = 2.48 \times 10^{-20}$, $I_e g = 1.06 \times 10^{-20}$, $\tau(\nu) = 5.0\nu^{-2.1}$, and ν , in this case, is frequency in MHz. I_g and I_{eg} are the coefficients obtained by Cane (Cane, 1979).

In (9), the first term applies to the galaxy contribution and the second term applies to extragalactic radio noise, which is considered spatially uniform.

This model can be simplified, according to (Ellingson, 2005), for frequencies above 10 MHz

$$I_\nu \approx I_g \nu^{-0.52} + I_{eg} \nu^{-0.80} \tag{10}$$

The Cane model for high frequencies is used in this work, underestimating the antennas performance. The Figure 3 shows that the T_{sky} is ranging from 300 000 K to 800 K between the frequencies of 10 MHz and 100MHz, respectively.

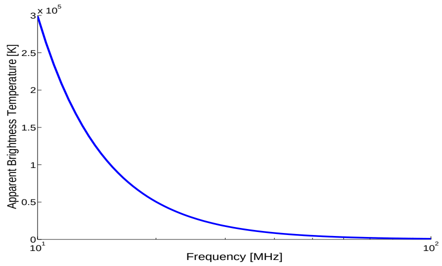

Figure 3: Apparent Brightness temperature received for a low gain antenna.

Useful Bandwidth

The main requirement for an active antenna is send a signal to the receiver, where the Galactic noise is dominant (Ellingson, 2005), hence it is necessary knowledge of the noise temperature system contributions. The Galactic noise temperature contribution is given by

$$S = e_r k T_{sky} (1 - |\Gamma|^2) G_{pre} G_f \tag{11}$$

Where S is the spectral Power density due to T_sky in the feed-line output, $[1 - |\Gamma|^2]$ is the fraction of power transferred from antenna radiator to the preamplifier, G_{pre}, is the preamplifier gain (in his work is used 32.5 dB for an average value of preamplifier gain), G_f is the coaxial cable loss and Γ is the voltage reflection coefficient. Γ at antenna output looking into the preamplifier is given by

$$\Gamma = \frac{Z_{pre} - Z_a}{Z_{pre} + Z_a} \tag{12}$$

According to (Ellingson, 2005), the ground radio noise can be neglected because it behaves more like a spotlight than as a body.

The man-made radio noise is the background radio frequency noise aggregate resulting from human activity, which is known to exhibit noise-like spectra. This radio noise is characterized in (International Telecommunications Union ITU-R Recommendation P.372-8, 2003) and applies a multiplication factor to the Galactic background radio noise. This radio noise is neglected in this work.

The instrumental noise can be divided into noise temperature contribution of the preamplifier and the transmission line N_p and N_f). They are defined by

$$N_{pre} = k T_{pre} G_{pre} G_f \tag{13}$$

and

$$N_f = k T_{phys} (1 - G_f) \tag{14}$$

Where T_{pre} is the preamplifier noise temperature and T_{phys} is the transmission line noise temperature.

Then, the galactic radio noise and instrumental noise radio ratio γ is given by

$$\gamma = \frac{S}{N_p + N_f} \tag{15}$$

NLTA Antenna

The Naval Research Laboratory LOFAR test array (NLTA) antenna, used, has as main advantages the fact that the dipole arms are wide with high mechanical resistance and low impedance compared to other antennas studied. However, it has copper volume of 11934 cm^3, and a mechanically complex structure. The simulated NLTA antenna followed the scale proposed by (Ellingson, 2005; Stewart et al, 2004), using a radiator with a radius of 16 mm.

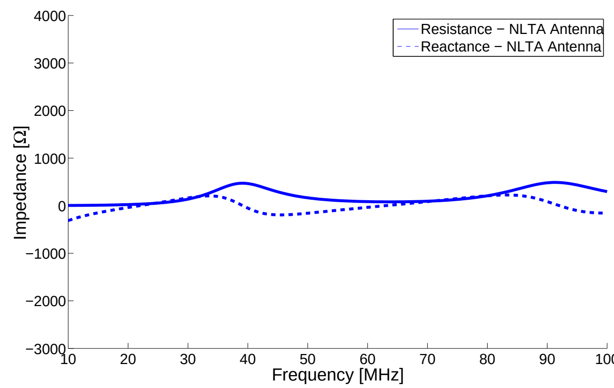

Figure 4: Simulated impedance characteristics for the NLTA antenna.

Inverted-V Dipole

The inverted-V dipole, used, has as main advantages, a mechanically simple structure and a low copper volume, 17.27 cm^3, but it presents high impedance outside the resonant frequency and low mechanical resistance. The simulated inverted-V dipole uses one arm of the dipole width of 2.75 m, a height of 2.4 m, an angle between the arms of 90 degrees, using the optimizations proposed by (Rosa, 2010b) and a radius of 1 mm.

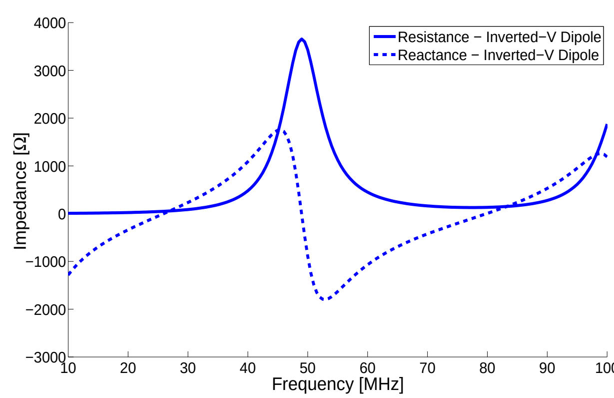

Figure 5: Simulated impedance characteristics for the Inverted-V dipole.

Fork antenna

The Fork antenna, used, has as main advantages, a mechanically simple structure, low copper volume, 47.1 cm^3, and low impedance compared to other studied antennas but it presents low mechanical resistance. The simulated Fork antenna uses one arm of the dipole width of 2.5 m, a height of 2 m, using the optimizations proposed by (Rosa, 2010b) and a radius of 1 mm.

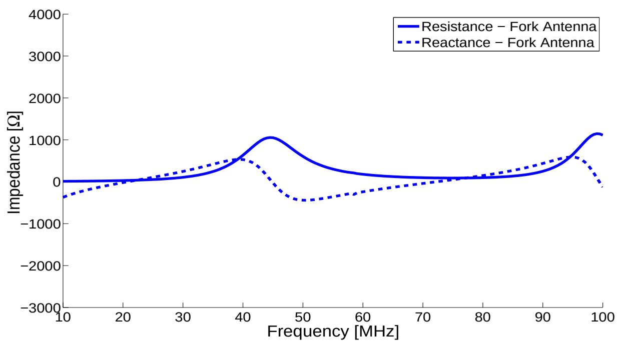

Figure 6: Simulated impedance characteristics for the Fork antenna.

Half-wavelength Dipole

The Half-wavelength dipole, with a resonant frequency of 50 MHz, used, has as main advantages, a mechanically simple structure and low copper volume, 9.1 cm^3, however, it presents high impedance outside the resonant frequency and low mechanical resistance. The simulated Half-wavelength dipole uses one arm of the dipole width of 1.45 m, a height of 2 m and a radius of 1 mm.

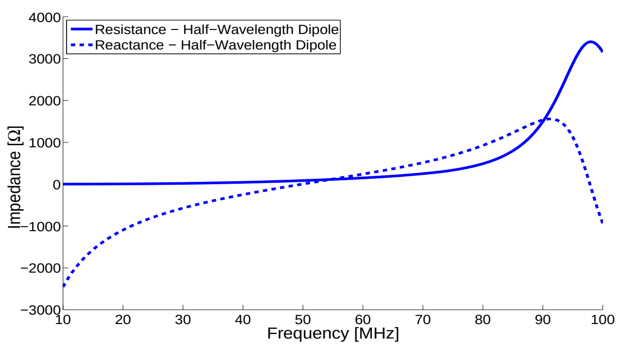

Figure 7: Simulated impedance characteristics for the Half-wavelength dipole.

Results

From the equations described in the previous section one can evaluate, in Figure 8, the frequency bandwidth in which the Galactic radio noise dominates the instrumentation radio noise (N_p and N_f) of active antennas.

The previous results are summarized in Figure 9, which shows the intensity of γ as a function of frequency for the voltage standing wave ratio (*VSWR*) simulated with the NEC-2 software, shown in Figure 10.

The Table 1 was constructed from the data presented at Figures 8 and 9.

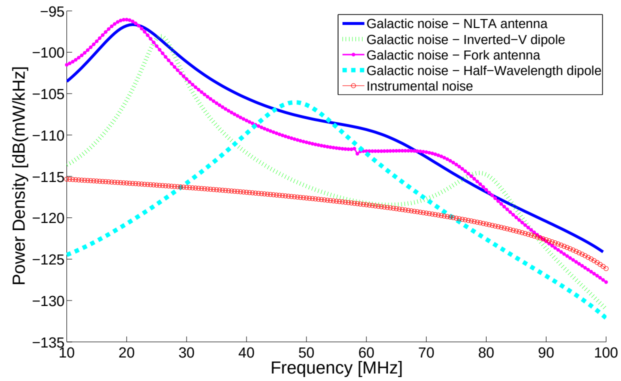

Figure 8: Power density at the receiver input to the antennas NLTA (dark blue), inverted-V dipole (light green), Fork (pink), Half-wavelength dipole (light blue) and instrumental radio noise (red).

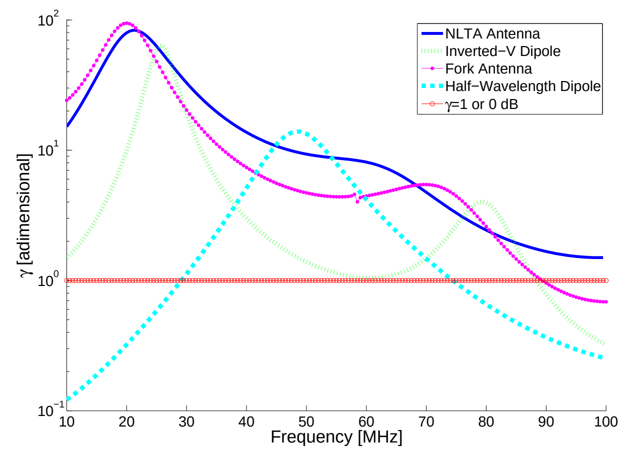

Figure 9: Comparison of $\gamma = 1$ (red) with γ calculated using the simulated *VSWR* for the antennas NLTA (dark blue), inverted-V dipole (light green), Fork (pink) and Half-wavelength dipole (light blue).

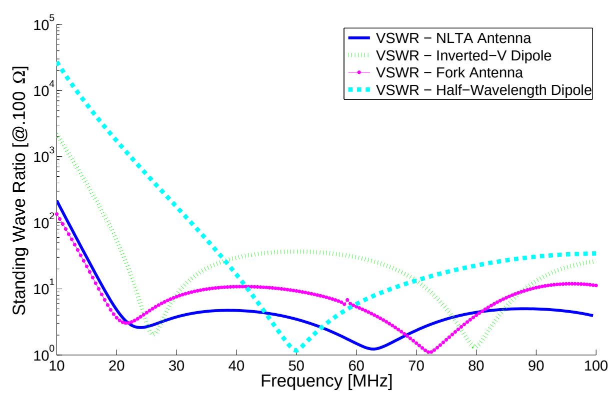

Figure 10: Standing wave ratio at the feed of the antennas NLTA (dark blue), inverted-V (light green), Fork (pink) and Half-wavelength dipole (light blue) to a normalized impedance of 100Ω.

Table 1: Relation between the antenna design and useful frequency bandwidth.

Antenna design	ν ($\gamma > 1$ $\in [10, 100]$) *MHz*	Δ ν *MHz*
NLTA	10 - 100	90
Inverted-V dipole	10 - 88.44	78.44
Fork	10 - 89.36	79.36
Half-wavelength dipole	29.12 - 74.43	45.31

Due to possible oscillations *S* or in (N_p and N_f) it is necessary that the antenna have a high useful bandwidth values stability, which is shown by Figure 11 considering oscillations of 6 and 10 dB. The Table 2 shows data from Figure 11.

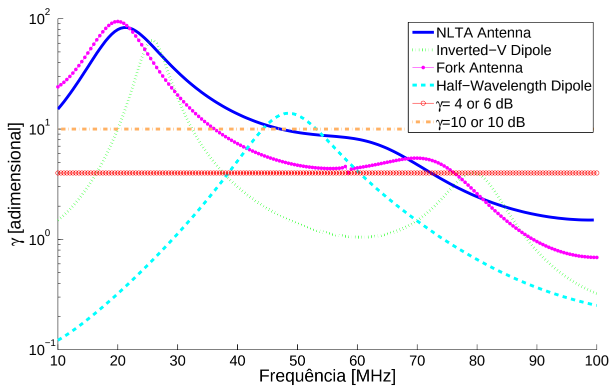

Figure 11: Comparison of γ = 4 (red) and γ = 10 (orange) with γ calculated using the VSWR simulated in software NEC-2 for the antennas NLTA (dark blue), inverted-V dipole (light green), Fork (pink) and Half-wavelength dipole (light blue).

Table 2: Value of the bandwidth useful for variations of 6 and 10 dB in γ.

Antenna design	ν ($\gamma > 4$ $\in [10, 100]$) *MHz*	ν ($\gamma > 10$ $\in [10, 100]$) *MHz*
NLTA	62.33	37.18
Inverted-V dipole	21.19	12.42
Fork	66.17	26.13
Half-wavelength dipole	21.91	8.91

The Table 3 was constructed adopting the copper density as 8.92 g/cm^3 and copper price of 9.564 US$/Kg, in the European market (Estadão, 2011). Table 4 lists the cost and useful bandwidth for each antennas design, ignoring oscillations.

Table 3: Value of the copper mass for each antenna design for its price in the European market.

Antenna design	*Mass kg*	*Price US$*
NLTA	106.45	1018.08
Inverted-V dipole	0.154	1.47
Fork	0.420	4.02
Half-wavelength dipole	0.081	0.77

Table 4: Relationship of bandwidth useful for the European market price for each antenna design.

Antenna design	$\Delta\nu(\gamma > 1$ $\in [10, 100])$ *MHz*	*Price US$*
NLTA	90	1018.08
Inverted-V dipole	78.44	1.47
Fork	79.36	4.02
Half-wavelength dipole	45.31	0.77

Conclusions

Analyses were performed for four possible antennas implementation, for a modern low frequency interferometric array. The antennas must present high frequency bandwidth dominated by Galactic radio noise, high useful bandwidth values stability, low cost and has a mechanically simple and resistant structure. Among the studied antennas The NLTA showed higher usable bandwidth, lower impedance and greater stability, but its price is approximately two hundred and fifty times more expensive than the other antennas, making their use impractical. The inverted-V dipole showed a low production cost and easy installation and a wide bandwidth dominated by the Galactic radio noise, but had low stability, which precludes their installation. The Fork antenna presents the best result among the four antennas designs analyzed, due to its low cost, high bandwidth dominated by Galactic radio noise and high stability. The Half-wavelength dipole was found to be an interesting alternative due to the lowest cost between the studied antennas designs, about five times less than the price of the antenna Fork, and a stability similar to the inverted-V dipole, even having a small bandwidth dominated by Galactic radio noise.

Acknowledgments

The authors thank the Program PIBIC/INPE - CNPq/MCT for the approval of the Research Project and the 12th CISBGf Organizing Committee for the opportunity to present our results.

References

ASTRON. (2011, Mar. 6). LOFAR [Online]. Available: http://www.astron.nl/general/lofar/lofar

Cane, H. V. Nov. 1979. Spectra of the non-thermal radio radiation from the galactic polar regions, Monthly Notice Royal Astronomical Society, vol. 189, pp. 465-478.

CAPPELLEN, W. A.; RUITER, M.; KANT G. W. 2007 Low Band Antenna: Architectural Design Document, ASTRON, LOFAR Project, Doc.id: LOFAR-ASTRON-ADD-009, ver. 2.1.

ELLINGSON, S.W. Aug. 2005. Antennas for the Next Generation of Low-Frequency Radio Telescopes, Antennas and Propagation. IEEE Transactions on Antennas and Propagation, vol.53, n.8, pp. 2480-2489,

ESTADÃO. (2011, Mar. 19). ESTADÃO [Online]. Available: http://www.estadao.com.br/estadaodehoje/20110318/not_imp693572,0.php

International Telecommunications Union ITU-R Recommendation P.372-8. Mar. 2007, Radio Noise.

LOFAR. (2011, Mar. 11). LOFAR [Online]. Available: http://www.lofar.org/

ROSA, G. S.; SCHUCH, N. J.; GOMES, N. R.; MACHADO, R. Dez. 2010a. Inexpensive Interferometer for Low Frequency Radio Astronomy. I2TS 2010. Rio de Janeiro, RJ. 13 - 15/12/2010.

ROSA, G. S. Dec. 2010b. Relatório de Estágio Supervisionado Laboratório de Ciências Espaciais de Santa Maria, Dept. Elect. Eng., Federal Univ. of Santa Maria, Brazil, Tech. Rep. presented as a Graduation Internship.

ROSA, G. S. Jul. 2010c. Desenvolvimento de Antenas, Receptores, Correlacionadores e Sistema de Aquisição de Dados para Interferômetro (20 - 80 MHz) de Baixo Custo – Radiointerferência, Dept. Elect. Eng., Federal Univ. of Santa Maria, Brazil, Tech. Rep. presented as a Graduation Monograph, Jul. 2010.

STEWART, K.P. et al. Dec. 2004. LOFAR antenna development and initial observations of solar bursts. Planetary and Space Science. vol. 52, Issue 15, pp 1351-1355.

TAN, G. H.; ROHNER, C. Jul. 2000. Low-frequency array active-antenna system, in Proc. SPIE, vol. 4015, pp. 446-457.